



Synthesis of non-enzymatic biosensor based on selenium dioxide nanoparticles in order to detection of glucose under electrochemical method

Neda Vahdani Parast Langeroudi¹, Abbas Mollataghi^{2*}

¹ Department of Physical Engineering, Faculty of Science, Qom University of Technology, Qom, Iran

² Department of Chemistry, Faculty of Science, University of Malaya, Kuala Lumpur, Malaysia

Abstract

In this project, a novel electrochemical biosensor was produced for the glucose recognition. Selenium dioxide Nanoparticle (SeNPs) synthesized a two-step process with a hydrothermal method. The SeNPs were characterized by X-ray diffraction (XRD). Also, the size distributions of nanoparticles were determined by dynamic light scattering (DLS), that more than 90 percent in the size range of 58–100 nm. The electrochemical performance of the SeNPs electrode for detection of glucose was investigated by cyclic voltammetry (CV). SeNPs show high electrocatalytic activity toward glucose oxidation in alkaline medium and are used for non-enzymatic electrochemical detection of glucose. The biosensor also had a linear response to glucose in the range of 0.5-2.5 mM and a low detection limit of 1.3 μ M glucose (S/N=3). Therefore, the sensor shows great promise for simple, sensitive, and quantitative detection and screening of glucose and real sample (glucose in the human serum). This novel structured electrode holds great promise for the development of biosensors and other electrochemical devices.

Keywords: biosensor glucose; selenium dioxide nanoparticle; non-enzymatic; glassy carbon electrode; cyclic voltammetry; electrochemical

Introduction

Nowadays the development of sensitive, selective, fast and reliable biosensors for detection of biomolecules is of almost importance for use in the biotechnology, bio-processing, clinical diagnostics, medical application, food industry and many other fields [1, 2]. Also in the development of renewable and sustainable fuel cells [2]. Comparing with other determination methods such as fluorescent, optical and electronic techniques, electrochemical techniques have been extensively applied due to their advantages as low cost, simple preparation, easy miniaturization and automation, high stability, etc [3]. Enzyme glucose sensors are based on the electrocatalysis of the enzyme glucose oxidase (GOx) to glucose oxidation. On the contrary, non-enzymatic glucose sensors which rely on the current response of glucose oxidation directly on the electrode surface. The performance of enzyme glucose sensors is susceptible to the chemical functional group and environmental factors including humidity, pH value and temperature due to the intrinsic nature of enzymes [4]. Although enzymatic sensors show high selectivity and sensitivity, the pursuit of non-enzymatic sensing with rapid response and precise measurement is a competitive area of research. Enzyme-free sensors can avoid some of the inevitable enzyme electrodes drawbacks such as the chemical and thermal instabilities originated from the intrinsic nature of enzymes without the need of immobilized enzyme on the sensor [5].

In recent years, various metal materials and their derivatives have been investigated for non-enzymatic biosensors [6] such as Co [7], Ni(OH)₂ [8], MnO₂ [9], have been broadly explored as the electrode modified-materials for developing non-enzymatic glucose sensors. However, these electrodes still suffer from inertia

behavior and surface contamination due to the absorption of intermediates and chloride ion [10] which result in poor operational stability of these biosensors. In recent years, researchers have shown an increasing interest in development of non-enzymatic glucose sensors based on metallic nanoparticles such as Pt [11], Pd [12], Pt/Pb [13] and Au [14], which showed some unique features including high specific surface area, improved electrocatalytic activity, good biocompatibility [15]. However, studies reveal that glucose oxidation on some noble metals including Pt and Au suffers from slow kinetics with decreased faradaic current [5]. The high price of noble materials and easy poisoning of their surfaces are also concerned. Therefore, there are increasing interests to use transition metals such as Ni, Cu, Ti, Co and Fe [16-18] for glucose sensing. Among various transition metals, nickel-based electrodes have been the most widely used sensors for the non-enzymatic determination [19]. NiO, CuO, CoO based non-enzymatic glucose sensors have been developed successfully in recent years by several groups [17]. Selenium dioxide has been proved as a promising material for non-enzymatic glucose sensing because of its low cost, chemical stability environmentally benign nature, relatively good conductivity and electro-catalytic property [20].

In this work, SeO₂ nanoparticles (SeNPs) were prepared by a two-step strategy, with a hydrothermal method. X-ray diffraction (XRD) and dynamic light scattering (DLS) analysis were applied to characterize the as-prepared sample. SeNPs modified electrode showed high catalytic activity for glucose electro-oxidation in alkaline medium. The effects of NaOH concentration and the applied potential were investigated and optimized. Cyclic

voltammetry (CV) detection of glucose was performed. Results show the proposed SeNPs exhibit high sensitivity and selectivity toward glucose detection and can be applied successfully in human serum.

Material and Methods

Chemicals

Selenium chloride hexahydrate ($\text{SeCl}_2 \cdot 6\text{H}_2\text{O}$), urea ($\text{CO}(\text{NH}_2)_2$), Nafion (5%) and D-(+)-glucose were purchased from Sigma–Aldrich. Glucose solutions with different concentrations were diluted from a stock solution (1 M). All the chemical reagents were used as received without further purification and all aqueous solutions were prepared with deionized water.

Preparation of SeNPs

SeNPs were prepared as follows. In brief, 0.59 g $\text{SeCl}_2 \cdot 6\text{H}_2\text{O}$ and 0.15 g $\text{CO}(\text{NH}_2)_2$ were dissolved in 20 ml distilled water and transferred into a 40 ml Teflon-lined autoclave, which was heated at 100°C for 12 h and then cooled to room temperature. The resulted pink precipitate was collected and washed with distilled water and absolute ethanol to remove the impurities. After this dried under vacuum at 60°C for 8 h. SeNPs were obtained by calcination of the resulting pink Selenium precursor nano-porous at 400°C for 2 h in air.

Preparation of SeNPs modified electrode

Before surface modification, a glassy carbon electrode (GCE) was polished with $1\ \mu\text{m}$ alumina slurries, and then rinsed thoroughly with deionized water and dried at room temperature. To prepare 5 mg/mL SeNPs suspension, 5 mg SeNPs was first dispersed in a mixture solution containing H_2O (500 μL), ethanol (490 μL) and Nafion (5%, 10 μL), and then sonicated for 1 h. After that, a 10 μL suspension was dropped onto the surface of GCE and dried naturally. The as-prepared electrode was denoted as SeNPs/Nafion/GCE. The Nafion coated GCE (Nafion/GCE) was also prepared with the same process as a control electrode.

Apparatus and electrochemical measurements

Powder XRD data were acquired on a Philips PW1730 diffractometer with $\text{Cu K}\alpha$ radiation ($\lambda = 1.54060\ \text{\AA}$). DLS measurements were performed on a HORIBA Jobin Yvon SZ-100 (Japan). All electrochemical measurements were performed on an Autolab EmStat3 electrochemical workstation (Netherlands). A typical three-electrode system was employed with a saturated Ag/AgCl as a reference electrode, a Pt wire as a counter electrode, and the SeNPs modified electrode as a working electrode. All electrochemical experiments were performed at room

temperature and all the potentials are reported against featured Ag/AgCl reference electrode. The solution was stirred to provide convective transport.

Result and discussion

Characterization of the SeNPs

SeNPs were obtained by calcination of corresponding Selenium precursor. The structure of the sample was determined by XRD analysis (Fig. 1). The Selenium precursor (green curve) show diffraction peaks indexed to $\text{Se}(\text{CO}_3)_{0.35}\text{Cl}_{0.2}(\text{OH})_{110}$ (JCPDS 38-0547) [21]. After calcination, only the diffraction peaks (red curve) of the SeO_2 phase are observed at 31° , 37° , 39° , 45° , 56° , 59° , and 65° , which are well indexed to (220), (311), (222), (400), (422), (511), and (440) planes of CuO (JCPDS 09-0418), indicating that the thermal decomposition and oxidization of this Selenium precursor causes its complete conversion to crystalline SeO_2 .

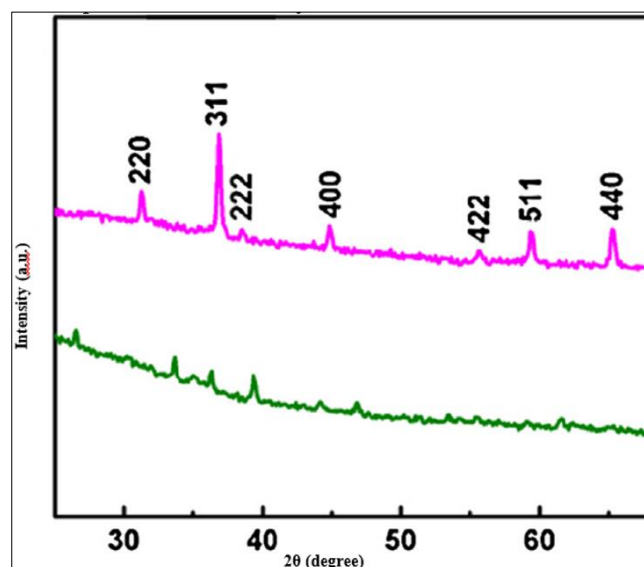


Fig 1: XRD patterns of $\text{Se}(\text{CO}_3)_{0.35}\text{Cl}_{0.2}(\text{OH})_{110}$ (green curve) and SeNPs (red curves).

Dynamic light scattering studies show a uniform size distribution of the SeNPs. The DLS pattern reveals that Selenium nanoparticles synthesized by a two-step process with a hydrothermal method have an average diameter of 99 nm (that more than 90 percent in the size range of 58–100 nm) with the polydispersity index (PDI) of 0.525.

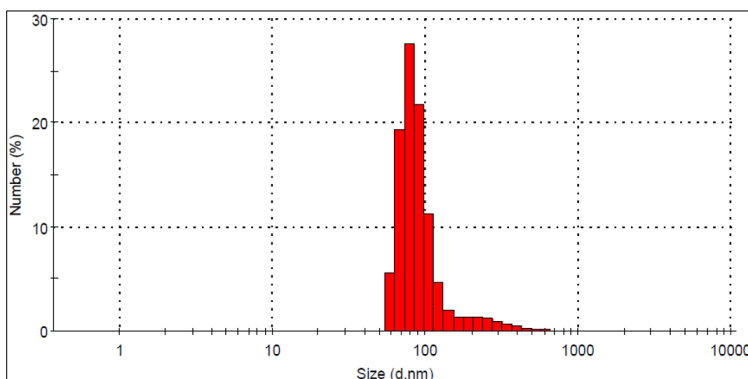


Fig 2: DLS patterns hydrothermal synthesized of SeNPs.

Electrochemical behavior of SeNPs/Nafion/GCE

The electrochemical behavior of SeNPs/Nafion/GCE was studied in 0.3 M

NaOH solution, and Nafion/GCE was also studied for comparison.

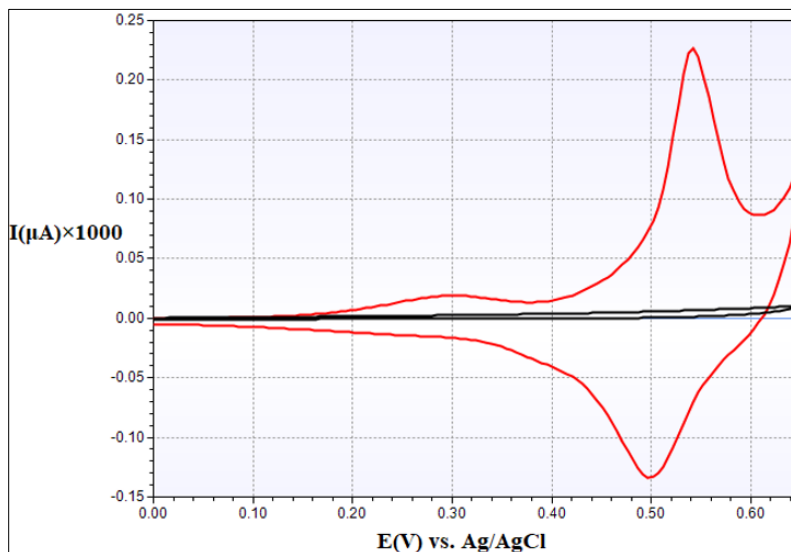


Fig 3: CVs of the Nafion/GCE (black curve) and SeNPs/Nafion/GCE (red curve) in 0.3 M NaOH solution.

Fig. 3 shows the CVs of the Nafion/GCE (black curve) and SeNPs/Nafion/GCE (red curve) in 0.3 M NaOH solution. No obvious oxidation or reduction peak was observed at Nafion/GCE. In sharp contrast, a pair of redox peaks can be

observed with the anodic peak at around 0.542 V and the cathodic peak at around 0.502 V at SeNPs/Nafion/GCE, which can be attributed to the reversible conversion between Co (III) and Co (IV) [22].

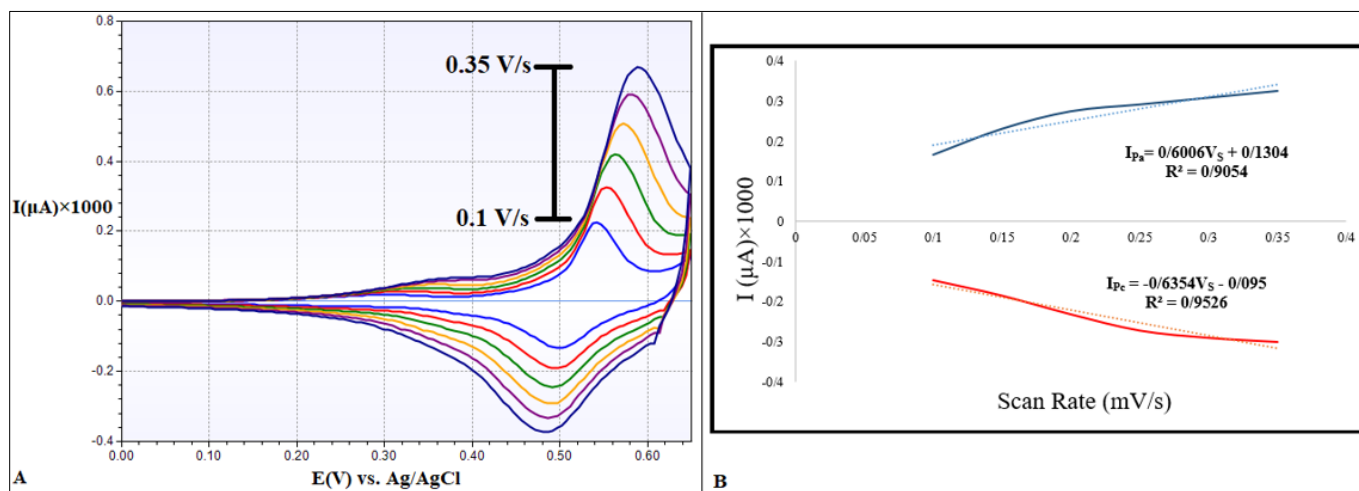


Fig 4: (A) CVs of the SeNPs/Nafion/GCE in 0.3 M NaOH at various scan rates of 0.1, 0.15, 0.2, 0.25, 0.3, 0.35 V/s.; (B) linear regression equations of peak currents vs. scan rate.

Fig. 4A shows the CVs of SeNPs/Nafion/GCE in 0.3 M NaOH solution at different scan rates.

With an increase of the scan rate, both anodic and cathodic peak currents increased.

Fig. 4B shows both of the redox peak currents increase linearly with the scan rate in the range from 0.1 to 0.35 V/s, suggesting a surface controlled electrochemical process of SeNPs/Nafion/GCE in alkaline solution. Linear regression equations: ($I_{pa} = 0.6006V_s + 0.1304$, $R_2 = 0.9054$; $I_{pc} = -0.6354V_s - 0.095$, $R_2 = 0.9526$). This indicates that the modified-electrode

reaction of glucose is a surface-confined process. In the scan rates ranging from 0.1 to 3.5 V/s, the linear regression equations of the E_{pa} and E_{pc} vs. the logarithm of the scan rates are expressed as $E_{pa} = 0.0332\ln V_s + 0.6165$ and $E_{pc} = -0.0156\ln V_s + 0.4669$ with $R = 0.9889$ and 0.9632 , respectively. Based on the slopes of the lines $RT/(1-\alpha)nF$ and $-(RT/\alpha nF)$, the value of the electron-transfer coefficient (α) and the electrontransfer number (n) were calculated as 0.56 and 1.

Electro-oxidation of glucose at the SeNPs/Nafion/GCE

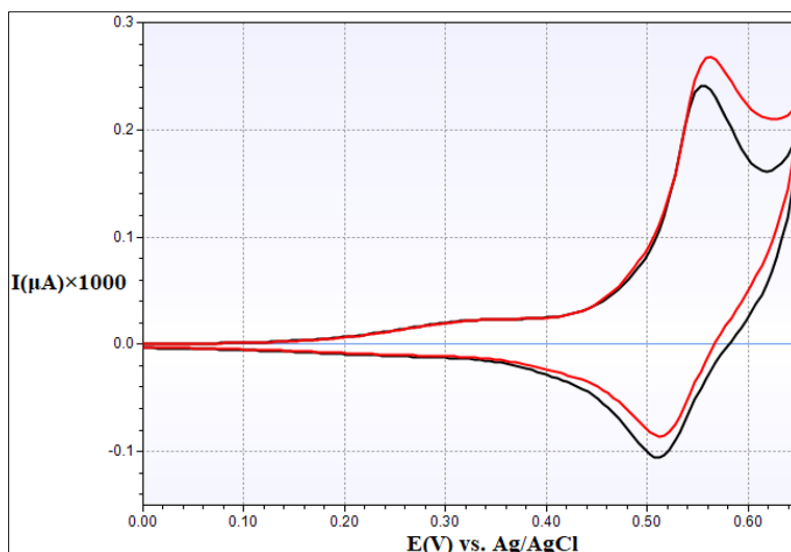


Fig 5: CVs of the SeNPs/Nafion/GCE in the absence (black curve) and presence (red curve) of 0.5 mM glucose in 0.3 M NaOH solution.

Fig. 3 shows the CVs of the SeNPs/Nafion/GCE in 0.3 M NaOH solution in absence of (black curve) and presence of (red curve) 0.5 mM glucose. Both an increased anodic peak current and a

decreased cathodic peak current were also observed upon addition of 0.5 mM glucose, suggesting the electrocatalytic activity of SeNPs/Nafion/GCE for glucose oxidation [23].

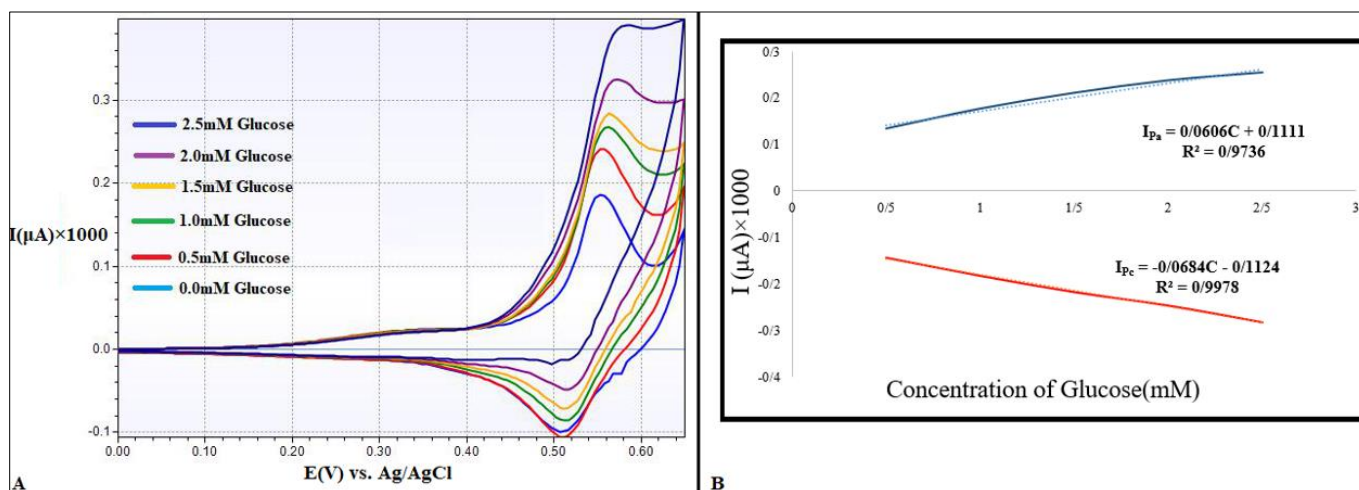


Fig 6: (A) CVs of the SeNPs/Nafion/GCE in 0.3 M NaOH upon addition of various concentrations of glucose.; (B) the linear regression equations of peak currents vs. concentration of glucose.

Fig. 6A shows the CVs of SeNPs/Nafion/GCE in 0.3 M NaOH solution containing the various concentration of glucose. The enhanced anodic peak current was observed with increasing concentration of glucose from 0 to 2.5 mM. In addition, an anodic shift in the peak potential from 0.565 V to 0.603 V was also observed. Such a slight shift in the anodic peak potential was reported to be attributed to the change in pH value due to the production of gluconolactone in the process of glucose electro-oxidation. Fig. 5B shows the dependence of the oxidation peak current (I_{pa}) of glucose on its concentration (C) was investigated in NaOH (0.3 M) solution.

The I_{pa} was linearly related to the glucose concentration in the range of 0.0–20 mM. The linear regression equation was $I_{pa} = 0.0606C + 0.1111$ with the correlation coefficient of 0.9736. The detection limit was 1.3 μM based on the signal-to-noise ratio of 3 (S/N=3).

Conclusion

Following a facile two-step procedure (synthesized a two-step process with a hydrothermal method), SeO_2 nanoparticles were fabricated. SeNPs show high electrocatalytic activity toward glucose oxidation in alkaline medium and are used as an effective sensor for glucose detection. These results make SeNPs a good candidate for the construction of a non-enzymatic glucose sensor in routine analysis.

References

1. Luqi K, Daiping H, Lili B. Nanoporous Selenium Dioxide nanowires for non-enzymatic electrochemical glucose detection, *Sensors and Actuators B: Chemical*, 2015, 888-894.
2. Mozhdeh M, Hossein A, Abdolreza S. Three-dimensional hybrid graphene/nickel electrodes on zinc dioxide nanorod

- arrays as nonenzymatic glucose, biosensors, *Sensors and Actuators B: Chemical*, 2017. <http://10.1016/j.snb.2017.05.062>
- Zongxu S, Wenyu G, Pei L, Xiaofang W, Qing Z, Hao W, *et al.* Highly sensitive non-enzymatic glucose sensor based on Nickel nanoparticle–attapulgitite-reduced graphene dioxide-modified glassy carbon electrode, *Talanta*, 2016. <http://dx.doi.org/10.1016/j.talanta.2016.06.016>
 - Hrapovic S, Luong J. Picoamperometric detection of glucose at ultrasmall platinum-based biosensors: preparation and characterization, *Analytical Chemistry*, 2003, 3308-3315.
 - Lu P, Liu Q, Xiong Y, Wang Q, Lei Y, Lu S. Nanosheets-assembled hierarchical microstructured Ni(OH)₂ hollow spheres for highly sensitive enzyme-free glucose sensors. *Electrochimica Acta*, 2015, 148-156.
 - Zhang B, He Y, Liu B, Tang D. Nickel-functionalized reduced graphene dioxide with polyaniline for non-enzymatic glucose sensing, *Microchimica Acta*, 2015:182:625-631.
 - Luo J, Jiang S, Zhang H, Jiang J, Liu X. A novel non-enzymatic glucose sensor based on Cu nanoparticle modified graphene sheets electrode, *Analytica Chimica Acta*, 2012:709:47-53.
 - Ji S, Yang Z, Zhang C, Miao Y, Tjiu W, Pan J *et al.* a Nonenzymatic sensor for glucose based on a glassy carbon electrode modified with Ni(OH)₂ nanoparticles grown on a film of molybdenum sulfide, *Microchimica Acta*, 2013:180:1127-1134.
 - Chen J, Zhang W, Ye J. Nonenzymatic electrochemical glucose sensor based on MnO₂/MWNTs nanocomposite, *Electrochemistry Communications*, 2008:10:1268-1271.
 - Ye S, Wen Y, Zhang W, Gan L, Xu G, Sheu F. Nonenzymatic glucose detection using multi-walled carbon nanotube electrodes, *Electrochemistry Communications*, 2004:6:66-70.
 - Chang G, Shu H, Huang Q, Oyama M, Ji K, Liu X. Synthesis of highly dispersed Pt nanoclusters anchored graphene composites and their application for non-enzymatic glucose sensing, *Electrochim Acta*, 2015:157:149-157.
 - Lin S, Chang S, Hsueh T. ZnO nanowires modified with Au nanoparticles for nonenzymatic amperometric sensing of glucose, *Appl Phys Lett*, 2014:104:193704.
 - Cui H, Ye J, Zhang D, Li C, Luong C, Sheu F. Selective and sensitive electrochemical detection of glucose in neutral solution using platinum–lead alloy nanoparticle/carbon nanotube nano composites, *Analytica Chimica Acta*, 2007:594:175-183.
 - Li Y, Niu X, Tang J, Lan M, Zhao H. A Comparative Study of Nonenzymatic Electrochemical Glucose Sensors Based on Pt-Pd Nanotube and Nanowire Arrays, *Electrochim Acta*, 2014:130:1-8.
 - Gao Z, Han Y, Wang Y, Xu J, Song Y. One-step to prepare self-organized nanoporous NiO/TiO₂ layers and its use in non-enzymatic glucose sensing, *Sci Rep*, 2013, 3.
 - Ding J, Sun W, Wei G, Su Z. Cuprous dioxide microspheres on graphene nanosheets: an enhanced material for non-enzymatic electrochemical detection of H₂O₂ and glucose, *RSC Adv*, 2015:5:35338-35345.
 - Ding Y, Wang Y, Su L, Bellagamba M, Zhang H, Lei Y. Electrospun Co₃O₄ nanofibers for sensitive and selective glucose detection, *Biosens Bioelectron*, 2010:26:542-548.
 - Mei H, Wu W, Yu B, Wu H, Wang B, Xia Q. Nonenzymatic electrochemical sensor based on Fe@Pt core-shell nanoparticles for hydrogen peroxide, glucose and formaldehyde, *Sens Actuators: B*, 2016:223:68-75.
 - Xu Q, Zhao Y, Xu J, Zhu J. Preparation of functionalized Selenium nanoparticles and fabrication of a glucose sensor, *Sensors and Actuators B: Chemical*, 2006:114:379-386.
 - Sattarahmady N, Heli H. A non-enzymatic amperometric sensor for glucose based on Selenium dioxide nanoparticles, *J. Exp. Nanosci*, 2012:7:529-546.
 - Chen X, Zhang Z, Qiu Z, Shi C, Li X. Hydrothermal fabrication and characterization of polycrystalline linnæite (Co₃S₄) nanotubes, 2009.
 - Zhou M, Zhai Y, Dong S. Electrochemical sensing and biosensing platform based on chemically reduced graphene dioxide, *Anal. Chem*, 2009:81:5603-5613.
 - Ding Y, Wang Y, Su L, Bellagamba M, Zhang H, Lei Y. Electrospun Co₃O₄ nanofibers for sensitive and selective glucose detection, *Biosens. Bioelectron*, 2010:26:542-548.